

Advances in High-Speed Design in
Dispersively Attenuating
Environments such as Cables &
Backplanes

Timothy Hochberg and Henri Merkelo
AtSpeed Technologies

Mike Resso
Agilent Technologies

2001 High-Performance System Design Conference

Abstract

This paper deals with advances made in methods for aiding the design and analysis of high performance digital networks that transmit information through dispersively attenuating paths such as cables and backplanes. The paper begins by discussing accurate, measurement based methods for determining dispersive attenuation characteristics (S_{21}), especially in the differential mode, and goes on to discuss techniques for predicting eye-pattern-diagram (EPD) waveforms and designing signal conditioning circuits. These methods are implemented as a set of software tools. Results from these methods are presented and discussed. Issues of cable design and skew are also discussed in the context of these results.

Introduction

Three new CAD tools for improving high-speed design in dispersive environments such as cables and backplanes are discussed herein. The capabilities of the tools are demonstrated by using them to illustrate some interesting high frequency, real-world phenomena of cables.

The first tool extracts dispersive attenuation characteristics (S_{21}) from time-domain transmission (TDT) data. The differential time domain data is acquired with the aid of a TDR/TDT instrument (such as Agilent #86100A with #54754A plugins). S_{21} is the ratio between the signal transmitted through a structure and the incident signal at a given frequency. In order to characterize dispersion accurately, both amplitude and phase of the frequency domain signals are taken into account. Therefore, the signals are treated as phasors and, correspondingly, S_{21} are complex quantities. See, for example, Ref. [1] for more information. This tool works in either single-ended or differential mode and can extract S_{21} data for the frequencies that correspond to the bandwidth of the TDT instrument. In practice, this limit is reached in the 10 to 12 GHz range. This compares extremely favorably to a conventional, two-port vector network analyzer (VNA) equipped with a balun for differential mode measurements since many baluns limit the useful frequency range of the instrument to ~ 2 GHz. Also, TDR/TDT measurement instruments are already available as standard equipment in many high-speed digital electronics laboratories; in those cases,

differential broadband characterization in the frequency domain requires only the software tool.

The second tool generates eye pattern diagrams (EPD) from S_{21} data. EPD are the metric of choice for determining the integrity of a signal path such as a cable and its attendant fixtures. The ability to generate EPD from S_{21} data removes the need for additional testing apparatus such as data pattern generators. It also allows many different structural configurations to be tested rapidly once the S_{21} parameters of the structures are determined.

One of the signal path components that can be included in the generated EPD is an equalization circuit. Equalization is the flattening of the frequency response of a cable. The high frequencies of the signal are generally more attenuated along the signal path than the low frequencies. For that reason, equalization is typically accomplished by some type of high pass filter. This reduces the magnitudes of the low frequency components of the signal so that they more closely match those of the high frequency components. Paradoxically, reducing the magnitude of some of the components of the transmitted signal can have the effect of increasing the magnitude of the opening in the EPD.

Once the type of equalization is decided, choosing the parameters of the circuit (e.g., R and C for an RC filter) may still involve a tedious search over a large parameter space. The third tool automatically chooses optimum values for filter parameters such as to maximize the area of the EPD. This allows rapid determination of a set of filter values and, in conjunction with the second tool, prediction of their effectiveness.

Broadband Determination of S_{21} in the Differential Mode

Only a limited number of methods exist for broadband characterization of components in the differential mode. The three available to the authors are shown in Table 1. The first, and most common is to use a conventional VNA with a balun. Unfortunately, baluns are generally limited to a bandwidth of ~ 2 GHz. Higher bandwidth baluns exist, but they are costly and produce measurements that are often subject to interpretation; there may be exceptions but they

were not available to the authors at the time of this writing. In general, now that cables and backplanes are routinely being designed for multi-gigabit applications, alternative methods for broadband determination of S_{21} in the differential mode are needed.

One alternative is offered by ATN Microwave [3,3]. They offer four-port VNA systems that can obtain S_{21} data up to 6 GHz or 20 GHz depending on the model. These systems are conventional vector network analyzers that are enhanced with ATN Microwave hardware and software.

A second alternative is discussed in this paper and, in more detail, in a companion paper that is also presented in this conference [2]. The method consists of extracting the S_{21} parameter from the TDT waveforms of a conventional TDR/TDT instrument such as Agilent model #86100A with #54754A plugins. It is shown that this method can routinely obtain S_{21} data up to 6 GHz in either single-ended or differential mode. With careful fixturing and attention to detail, data can be obtained up to the bandwidth of the instrument, which is in the 10 to 12 GHz range. This method, therefore, falls between the two ATN Microwave solutions in terms of frequency range, as show in Table 1. However, since the TDR/TDT instrumentation is frequently already available in high-speed digital electronics laboratories, only the software itself is needed in order to perform the evaluation and design demonstrated in this paper.

As mentioned earlier, the details of the extraction method are discussed in a companion paper. The following section contains examples of S_{21} data extracted using this method as well as discussions of some issues raised by the extracted S_{21} parameters.

Examples of S_{21}

The S_{21} data, both loss and phase, associated with a 22-AWG (American Wire Gauge) quad cable are shown in Figure 1 and Figure 2. This cable is interesting because its deviation from the shape of a typical loss curve is especially dramatic; the loss is more than doubled in some of the peaks. The TDT data from which this S_{21} data is extracted is shown in Figure 3. Although the peaks have the characteristics of resonances, the effect is actually due to periodic

discontinuities in the cable and is similar to the phenomenon of Brag reflection seen in crystals. This is discussed in the sidebar *Periodic Discontinuities and S_{21}* .

As another example, the loss portion of the S_{21} data for a 2.64 m length of 26 AWG differential cable is shown in Figure 4. Two curves are shown. The blue curve corresponds to the intrinsic attenuation of the cable. The red curve, which exhibits a large loss that peaks around 3.5 GHz, corresponds to the same cable when 167 ps of skew are introduced. The data without skew is typical for the loss curve of a well-designed cable. By contrast, the data for the cable with skew shows how dramatically skew can affect S_{21} and thus signal integrity. The origins of the loss associated with skew are discussed in the sidebar *Skew and S_{21}* .

Table 1: S_{21} determination methods

Method	Range
VNA plus balun	2 GHz
ATN Microwave #4001	6 GHz
TDT extraction	10 GHz
ATN Microwave #4002	20 GHz

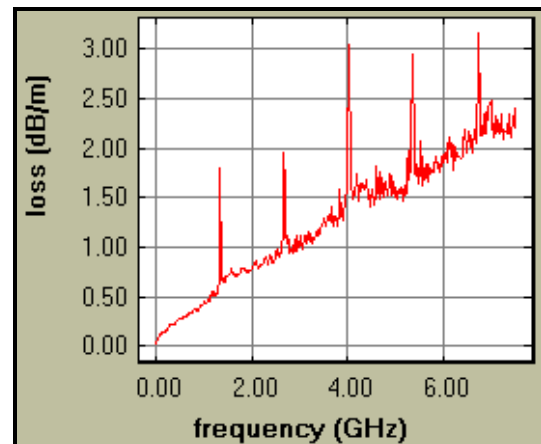


Figure 1. Plot of the loss component of S_{21} for a differential pair of a 22 AWG quad cable. The data is obtained from the TDT waveforms shown in Figure 3.

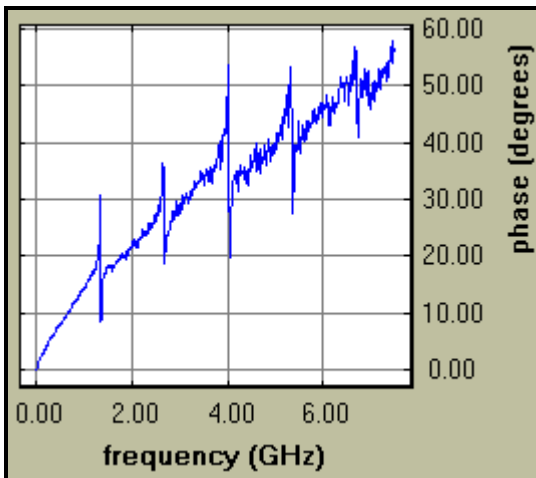


Figure 2. Plot of the phase component of S_{21} for a differential pair of a 22 AWG quad cable. The data is obtained from the TDT waveforms shown in Figure 3.

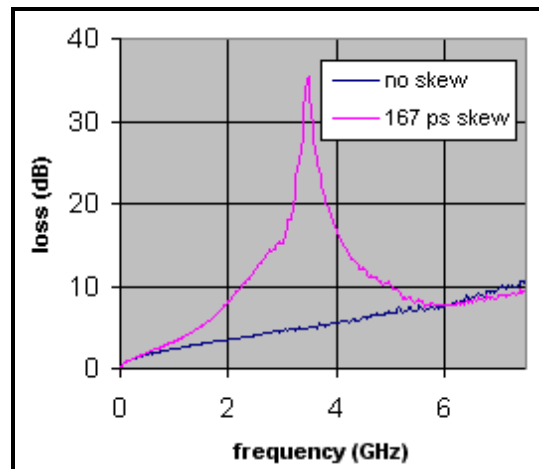


Figure 4. Loss data for a 2.64 m, 26 AWG, differential cable with and without skew.

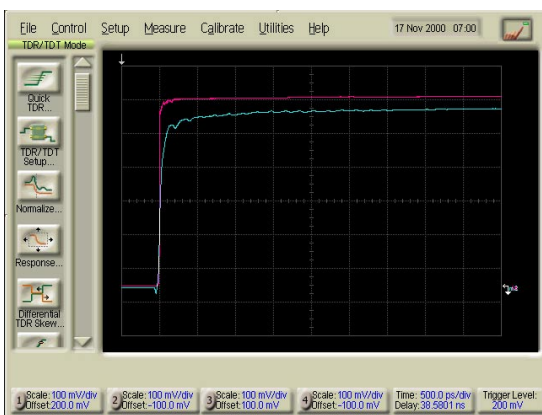


Figure 3. TDT waveforms measured through a differential pair of 11.7 m, 22 AWG quad cable. The blue curve corresponds to TDT through 11.7 m of cable while the red corresponds to TDT through the fixturing alone.

Periodic Discontinuities and S_{21}

Consider a transmission line with periodic discontinuities every Δx along the line. At frequencies satisfying:

$$f = \frac{nv}{2\Delta x} \quad n = 1, 2, 3, \dots$$

The reflections from the discontinuities are in phase and the reflection from the cable approaches 100%. (v is the velocity of propagation on the transmission line). This is known as the Bragg condition in the X-ray crystallography field. The peak in reflection will obviously correspond to a loss peak in the S_{21} parameters of the line.

Periodic discontinuities are common in cables. One frequent source of discontinuities is the cable shielding. Many cables have a metallized plastic shield that wraps the cable core. This results in a discontinuity in the cable with Δx equal to the pitch of the shield wrapping. If the pitch is greater than ~ 2 cm, the first peak in the loss curve is located below 5 GHz, where it may affect contemporary network design.

Figure 1 shows a particularly dramatic example of this effect. This effect has been seen in other measured cables, but typically at somewhat higher frequencies and never with peaks of this sharpness. The differing sharpness of the peaks presumably has to do with how well the pitch of the shield is controlled during the cable manufacture.

Skew and S_{21}

Skew can have a dramatic effect on S_{21} as shown in Figure 4. Skew has the effect of transferring energy from the differential (odd) mode to the even mode at certain frequencies. In particular, all of the energy is transferred to the even mode when the frequency f satisfies:

$$2f\Delta t = 1 + 2n, \quad n = 0, 1, 2, \dots$$

where Δt is the skew. At these frequencies, the relative phase of signals travelling on the two signal lines shifts by 180° . Thus, a differential signal that starts with opposite polarities on the two lines of a differential pair ends up arriving at the receiving end with equal polarities. This corresponds to a complete transfer of energy from the odd (differential) to the even mode. Note that, conversely, even mode signals are transformed into differential mode signals at these same frequencies, which can also cause problems.

S_{21} , including skew, can be written as:

$$S_{21}^{skew} = \cos(\pi f \Delta t) S_{21}^{noskew}$$

This matches the shape of the curve seen in Figure 4 quite well. However, for a skew of 167 ps, the expected location of the peak is 3 GHz while the observed location is at 3.5 GHz. The observed shift is likely due to the presence ~ 24 ps of skew present in the cable before skew is added.

EPD Generation from S_{21}

It is possible to generate the EPD associated with a cable and its attendant terminations from its S_{21} characteristics alone if some modest assumptions are made. The use of measured S_{21} to generate the EPD avoids issues of validity of the transmission line model. Generating S_{21} allows the rapid investigation of the effects of bit rate, cable length and terminations on the EPD. Both time and expense are saved by avoiding repeatedly fixturing and measuring different cable configurations.

Eye pattern diagrams are generated using the model shown in Figure 5. The transmission line is characterized by its S_{21} parameter. The equalization circuit (Eq) and load are arbitrary except that they are linear. The two primary simplifications of this model are the matched source and the linearity of all components. Linearity greatly simplifies the computation since nonlinear solution techniques need not be used. The matched source assumption simplifies

the model since internal reflections can be neglected.

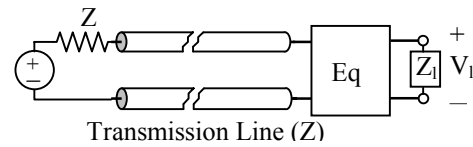


Figure 5: Model used to generate EPD.

For many cases, loads are sufficiently close to linear such that this model is satisfied. Mismatches at the source also do not seriously affect the model as long as the quantity $\Gamma_s \Gamma_l S_{21}^2$ is small. Here Γ_s and Γ_l are the reflection coefficients at the source and load, respectively. In the case of long cables or high speeds where EPD are most useful, this is generally satisfied.

The EPD is generated by first constructing a time domain voltage waveform $v(t)$ from a finite length bit sequence such as K28.5. This represents the waveform at the source and includes the effects of the finite signal risetime. The Fourier transform of $v(t)$ is represented by $V(\omega)$. The voltage at the load is then given by $V_l = (1 + \Gamma_l) S_{21}^{eq} S_{21}^{DUT} V$. Γ_l is the reflection coefficient from the equalization and load, while S_{21}^{eq} and S_{21}^{DUT} are the transmission coefficients of the equalization circuit and transmission line respectively. V_l is transformed back to the time domain and plotted to obtain the EPD.

By way of examples, generated EPD for the 22 AWG cable and 26 AWG cable without skew that were discussed previously are shown in Figure 6 and Figure 7, respectively. The sequence used in these examples is a pseudo-random bit stream of length $2^7 - 1$. Generation of these and similar EPD takes only a few seconds on an average performance PC. This allows many EPD to be evaluated rapidly for many different rates and cable lengths. When shorter bit patterns, such as K28.5, are used, pattern generation takes well under a second.

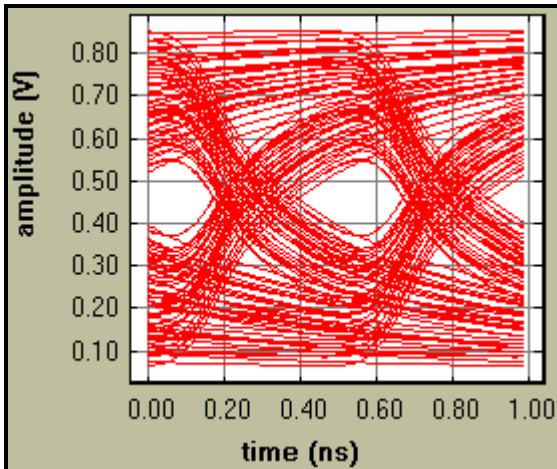


Figure 6. EPD at 2 Gb/s data rate propagated through 12 m of a 26 AWG differential cable.

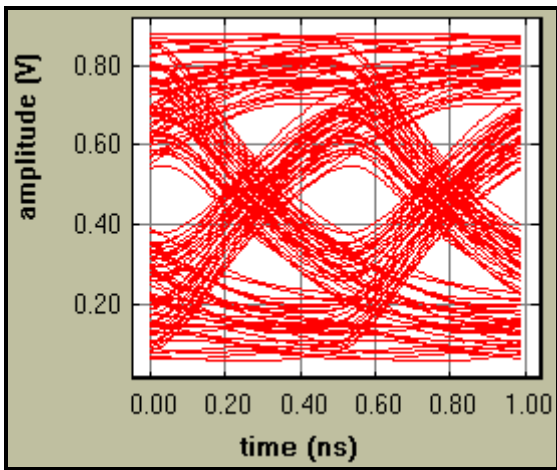


Figure 7: EPD at 2 Gb/s data rate propagated through 24 m of a 22 AWG differential cable.

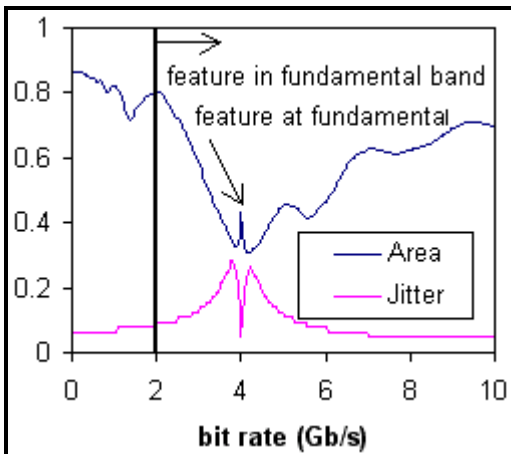


Figure 8. Plot of the open eye area and jitter versus bit rate for the S_{21} shown in Figure 9.

S_{21} Features and EPD

The frequency components of a random bit stream consist of a series of bands separated by nulls as shown in Figure 9. The first band, the principal band, extends from 0 Hz up to the bit rate. Note that this band extends well above the so-called fundamental frequency of the bit stream, which is equal to half of the bit rate. The principal band is also filled with a rich subharmonic spectrum. The characteristics of the EPD are primarily due to the properties of S_{21} in the principal band.

This point is illustrated in Figure 8 where EPD eye opening area and jitter are plotted as a function of bit rate for a signal that is propagated through a transmission line characterized by the S_{21} curve shown in Figure 9. This S_{21} curve has a characteristic resonance feature centered at 2 GHz. Effects on skew and jitter occur primarily when the center of the feature is within the principal band and are particularly apparent when it is near the fundamental itself.

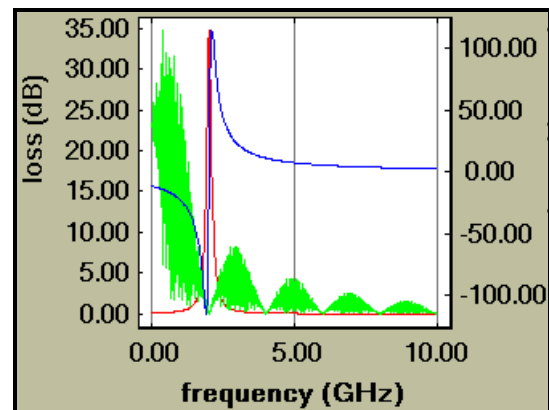


Figure 9. Plot of the S_{21} characteristic that is used to generate Figure 8 (phase, blue; loss, red). The magnitude of the frequency spectrum of a 2 Gb/s pseudo-random bit stream of length $2^{10}-1$ bits is also shown (green). The magnitude of the spectrum is in arbitrary units and is shown on a linear scale.

Equalization

Equalization is the use of a filter to flatten the frequency response of a propagation channel, whether it is a cable or a circuit board or both. A simple RC filter is often sufficient to dramatically improve the EPD when the correct filter parameters are chosen. An example of equalized transmission is shown in Figure 10.

Given the ability to generate EPD numerically, it is possible to determine optimum values for the components of an equalization circuit automatically, provided a suitable metric can be formulated. The open eye area is a metric that works well, although other criteria, such as eye height or minimum jitter, can also be used. Since EPD are generated many times during the course of the optimization, it is essential that the EPD generation is rapid. Fortunately, the EPD scheme discussed previously is extremely fast. Even so, the optimization is limited to short bit patterns such as K28.5.

Examples of Optimized Equalization

The EPD shown earlier for the 22 and 26 AWG cables are recomputed with equalization implemented with RC filters. The values of the circuit components for the filters are determined automatically. The results are shown in Figure 11 and Figure 12. In both cases, there is dramatic improvement in both the size of the eye opening and in the amount of jitter. The improvement in jitter is larger in the 26 AWG case, probably because of the relative smoothness of its S_{21} .

As these examples show, equalization is a powerful tool for improving the performance of lossy, dispersive channels. In both of the examples discussed, the eye opening is approximately doubled in height. The jitter is also dramatically reduced; in the 26 AWG case, almost eliminated.

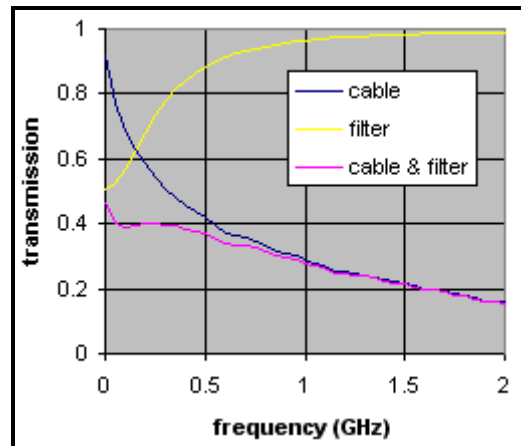


Figure 10. Transmission through a 26 AWG differential pair equalized for 2 Gb/s data rate

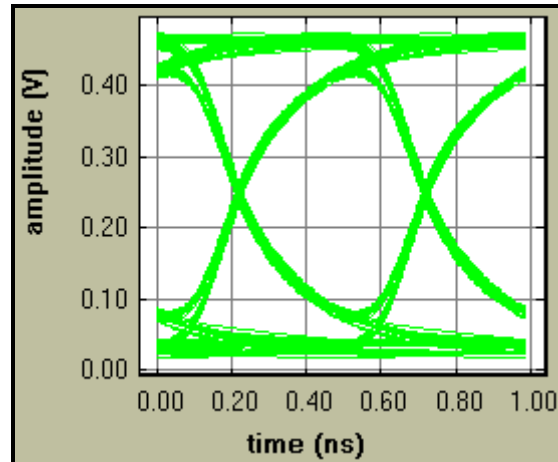


Figure 11. EPD of a 2 Gb/s data propagated through 12 m of equalized 26 AWG differential cable.

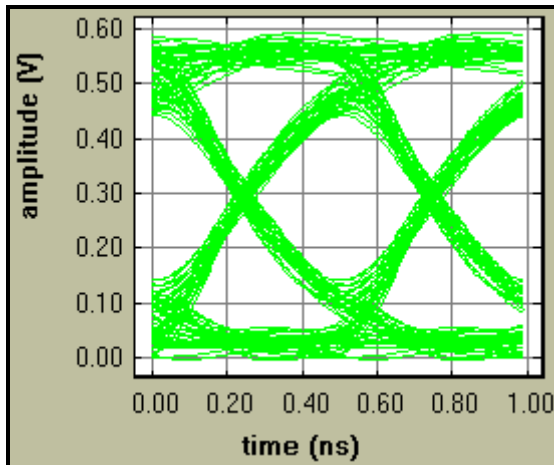


Figure 12: EPD of a 2 Gb/s data propagated through 24 m of equalized 22 AWG quad differential cable.

Summary and Conclusion

As serial digital speeds increase, data in backplanes and cables are particularly prone to undergoing unequal damping and dephasing. These effects lead to serious eye pattern degradation in the form large amplitude fluctuations and pronounced jitter. Three tools that ease the evaluation and design in such lossy, dispersive environments are presented. The first tool extracts the S_{21} parameters, both amplitude and phase, from TDT data at frequencies of up to 10 GHz. Extraction works equally well in both single-ended and differential modes. The second tool generates EPD from S_{21} data and includes the effects of mismatched terminations and equalization. The last tool finds and optimizes the parameters of equalization filters. In combination, these tools provide a designer the means to develop products and evaluate their performance when signal degradation is dominated by loss and dispersion. What's more, is that with these tools, minimal equipment is needed; only TDT measurement hardware is required and it is often already available in the digital design environment.

References

1. V.Valkenburg, ed. *Reference Data for Engineers: Radio, Electronics, Computer and Communications*, 8th edition. Boston: Newnes, 1998, pp 31-1–31-31.
2. T. Hochberg et al. "Broadband Measurements in the Differential Mode:

Accurate Determination of Dispersive Attenuation." *DesignCon 2001*, Santa Clara, CA, January 29 2001.

3. "The ATN-4000 Series Multiport and Differential S-Parameter Systems."
<http://www.atnmicrowave.com/multi/multi.html>